Weather and Climate Extremes 27 (2020) 100193

Contents lists available at ScienceDirect

Weather and Climate Extremes

journal homepage: www.elsevier.com/locate/wace

Climate extremes and agricultural commodity markets: A global economic analysis of regionally simulated events

Thomas Chatzopoulos[a,*], Ignacio Pérez Domínguez[a], Matteo Zampieri[b], Andrea Toreti[b]

[a] European Commission, Joint Research Centre (JRC), Inca Garcilaso 3, 41092, Seville, Spain
[b] European Commission, Joint Research Centre (JRC), Via Enrico Fermi 2749, I, 21027, Ispra, Italy

ARTICLE INFO

Keywords:
Climate extremes
Weather extremes
Agricultural commodity markets
Simulation

JEL classification:
Q11
Q17
Q18
Q54
Q56

ABSTRACT

Agroclimatic extremes can be seen as typical supply shifters that, on a par with economic and structural drivers, distort supply, demand, trade, and induce price variability. Economic simulation models typically operate under the assumption of 'normal' growing conditions, contain no explicit parameterization of climatic anomalies on the supply side, and confound multifarious sources of yield fluctuation in harvest-failure scenarios. In this article we follow a novel approach by augmenting a partial equilibrium model of global agriculture with a recently developed indicator of yield stress. We perform a multi-scenario analysis where the most extreme temperature and soil-moisture anomalies of the last decades, be it negative or positive, recur in the near future. Our results indicate that: *(i)* regional climate extremes may have significant economic impacts both at the domestic and international levels; *(ii)* the magnitude of the transmission effect depends on the attributes of the simulated extremes, the positioning of the impacted country in the trade arena, and the market status quo at the time of the shock; and *(iii)* crop prices generally display asymmetry to the direction of the agrometeorological shock with stronger responsiveness to negative anomalies (i.e., those leading to yield reduction) than to positive ones.

1. Introduction

Over the last decades we have witnessed meteorological extremes of unprecedented frequencies, intensities, and duration (IPCC, 2012). Especially during the 2000s, the warmest decade on record since 1850, numerous regional and global records were broken (WMO, 2013). The Fifth Assessment Report of the Intergovernmental Panel on Climate Change (IPCC) leaves little room for doubt on the future occurrence of extreme climatic anomalies. Large-scale events such as the 2003 European heatwave and the 2010 and 2012 droughts in Russia and the US will *'very likely'* occur more frequently, more intensely, and last longer (IPCC et al., 2012).

Climate extremes are increasingly expected to collide with major drivers that already put pressure on the global food system such as population growth, dietary shifts, environmental degradation, and trade interdependence (Janetos et al., 2017). For this reason, the impacts of adverse crop-growing conditions on supply and demand gain a honorable mention in agricultural outlook and market reports (e.g., OECD/FAO, 2018, Chinese Ministry of Agriculture, 2016; Trostle, 2008). A recently published simulation example can be found in the 2017 EU Medium-Term Agricultural Outlook where it was shown that extreme events during the growing season in various EU Member States may significantly affect domestic grain prices (European Commission, 2017). Paradoxically enough, the impacts of extreme events on the agricultural sector constitute an area considerably under-researched than climate change itself, on which integrated assessments, scenario harmonization, and model intercomparison have recently started to make a step change (Nelson et al., 2014). To our knowledge, there is no peer-reviewed study that assesses the sensitivity of agricultural markets to climate extremes. In addition, recent work seems to overlook the short-to-medium term effects of localized extremes by placing emphasis on the longer-term role of global events (Janetos et al., 2017; Araujo-Enciso et al., 2015a; Bailey et al., 2015; Fuss et al., 2015). Meteorological extremes and food systems are inherently local, and therefore understanding the long-term agricultural impacts of global extremes (e.g., El Niño) can benefit from the decomposition of the short-to-medium-term impacts of regional events.

In this article we aim to fill the above gap by 'stress-testing' the agricultural sector with extreme agroclimatic shocks. More specifically, we set out to quantify the potential domestic and global market impacts of combined events that may occur in key growing areas of three major crops: wheat, maize, and soybean. We pursue this assessment by means of incorporating a recently developed indicator of compound yield stress into a global partial equilibrium model of agricultural markets

* Corresponding author.
E-mail address: thomas.chatzopoulos@ec.europa.eu (T. Chatzopoulos).

https://doi.org/10.1016/j.wace.2019.100193
Received 6 April 2018; Received in revised form 31 October 2018; Accepted 8 January 2019
Available online 30 January 2019

and policies. Ultimately, we simulate 58 single region-crop-year deterministic scenarios to explore how agricultural commodity markets may react if past extreme events were to recur in the near future.

The work underlying this article adopts an innovative approach in the line of impact studies. The potential effects of climate- or weather-related phenomena are typically modelled with the implementation of historical yield or production shocks into the future (Araujo-Enciso et al. 2015a, 2017; Lunt et al., 2016; Fuss et al., 2015; Bailey et al., 2015; Wiebe et al., 2015; Willenbockel, 2012). The downside of the so-called 'supply-shock approach', albeit straightforward to implement and easily tailored to allow for scenario harmonization and model intercomparison, is that it cannot deal with the attribution of crop price variability in the context of extreme events. Crop yield fluctuations and the subsequent price variability may be the immediate or lagged result of a mix of short- and medium-term factors such as speculation, pest or disease outbreaks, domestic policies, structural change, and macroeconomic conditions, all on top of changing agrometeorology and evolving agricultural systems. In most large-scale partial or general equilibrium models, where the focus is typically on economic and structural drivers of yields, the magnitude of production oscillations falls short of attributing the extent of commodity price fluctuations to adverse growing conditions (Baffes and Haniotis, 2010). For this reason, the attribution of yield cutbacks to adverse meteorology is often done on the basis of subjective judgment and (over-reported) media news that take the place of an empirical justification of the spatio-temporal attributes of the underlying phenomena (see Marx and Weber, 2012).

Incorporating an empirical index that summarizes the regional sensitivity of crop yields into a global economic model disentangles the above caveats. Furthermore, our approach takes into perspective key factors that determine the magnitude of market impacts of an extreme event, and therefore can be seen as a stylized alternative to the more classic integrated approach. More specifically, our composite stress index considers both the historical sensitivity of the affected areas to extreme events (e.g., through agronomic practices) and the attributes of those events, such as relevance, timing, intensity, and spatial coverage. Using a global agricultural model ensures that agricultural policies (e.g., prioritization of grains for domestic use), governmental protectionism (e.g., case of the Russian export ban following the 2010 drought), and trade positions are mathematically represented, while exploiting recent medium-term projections ensures that the status quo of, and expectations for, key crop markets are up to date.

Weather and climate extremes can be defined in various ways (Sillmann et al., 2017, National Academies of Sciences, 2016; Stephenson, 2008). Weather extremes generally signify rare and short-lived events, generally lasting from hours up to several days, with devastating potential. Typical examples are very hot days and heavy rains. Climate extremes represent similar events but viewed over longer periods such as weeks or months. The index used herein is based on meteorological anomalies that exert biophysical stress in specific time windows during the growing season. Henceforth, we adopt the term 'climate (or agroclimatic) extremes'. It is important, however, to recognize that a thin moving line separates climate from weather; 'thin' because a persistent or large-scale weather extreme is essentially a climate extreme, and 'moving' because a shift in the broader climate system changes the way we perceive and define either term (see the classic distributional shifts in IPCC et al., 2012, p.41).

The remainder of this article is organized as follows. An introduction to the stress index, its incorporation into the global agricultural model, and backdrop on the simulation scenarios are given in Section 2 (Methods). A compilation of results from our simulation experiment with the focus on production, trade, and prices is provided in Section 3 (Results). We conclude with study limitations, an outline of ongoing work on stochastically simulated extreme events, and suggestions for future research (Section 4).

2. Methods

2.1. Combined Stress Index (CSI)

The CSI, originally developed in Zampieri et al. (2017), is a descriptive indicator of historical agroclimatic extremes. It is a composite index that attributes yield anomalies –that is, deviations from a baseline trend– to climatic stress throughout the period 1980–2010. The CSI is based on the superposition of two other indices, a temperature-anomaly index that captures heat stress and a soil-moisture index that quantifies persistent water stress, on average national yields:

$$YLD_{r,c,t} \sim CSI_{r,c,t} = \hat{\alpha}_{r,c} \times HMDI^{det,std}_{r,c,t} + \hat{\beta}_{r,c} \times SPEI^{det,std}_{r,c,t} \tag{1}$$

where HMDI is the Heat Magnitude Day Index, SPEI is the Standard Precipitation Evapotranspiration Index, r, c, and t are region, crop, and year identifiers respectively, while *det* and *std* denote detrending and standardization. The alpha and beta coefficients are ridge-regression estimates that reflect the relative contribution of each stressor to yield anomalies. By construction, positive CSI values indicate limiting conditions for crop growth that stem from 'single' climatic anomalies such a heatwave *or* a drought, or combined events such as a heatwave *and* drought. Similarly, negative CSI values denote temperature and soil-moisture conditions that induce yield improvement. Zero or near-zero CSI values reflect close-to-average ('normal') agroclimatic conditions with respect to the baseline yield trend.

The multidimensional nature of extreme events renders their complete description by a single number rather complex (Stephenson, 2008). The overall attractiveness of the CSI lies in the coverage of multiple meteorological attributes. Non-zero values, for instance, reflect the *occurrence* of climatic anomalies that lead to yield anomalies. The temperature counterpart of the CSI (HMDI) accounts for the *frequency* and *amplitude* of abnormally high daily temperatures. The CSI is computed for the phenologically most critical months of each crop after planting (*timing*); that is, two months before the harvest of wheat and soybean, and four to two months before the harvest of maize. These time windows include anthesis and grain filling, shortly before and during which extremes lead to parthenocarpy and grain deformation (Luo, 2011; Porter and Gawith, 1999). Finally, the CSI focuses exclusively on agricultural regions and accounts for multiple cropping (*spatial coverage*). The joint consideration of the aforelisted attributes leads to statistically significant correlations between regional CSI's and year-to-year variability of yields in the vast majority of cases (Fig. 1). At the global level, the CSI for wheat explains over 40% of the year-to-year yield variability (Zampieri et al., 2017) while the CSI for maize goes even higher (> 50%; own estimation). Sometimes the impact may even be systematically visible on international reference prices, especially when large-scale extremes affect big exporters or importers (Fig. 2).

2.2. The economic model

Aglink-Cosimo is a global recursive-dynamic partial equilibrium model of agricultural commodity markets. It is the main modelling tool used in the OECD-FAO Agricultual Outlook that comprises medium-term projections for counterfactual policy analysis, issued every summer (OECD/FAO, 2018). A similar exercise is carried out by the European Commission at the end of the year upon extending the OECD-FAO baseline with EU short-term updates, alternative macroeconomic assumptions, and expectations of market experts (European Commission, 2017). The model is developed and maintained by the OECD and FAO Secretariats with a defined group of users from national agencies and research institutes, including the JRC.

Aglink-Cosimo covers over 90 commodities in 44 countries and 12 regions, and performs supply, demand, trade, and price simulations over a 10-year horizon. The model is trend-, elasticity-, and expert-driven, consists of over 43,000 linear or linearized behavioral equations

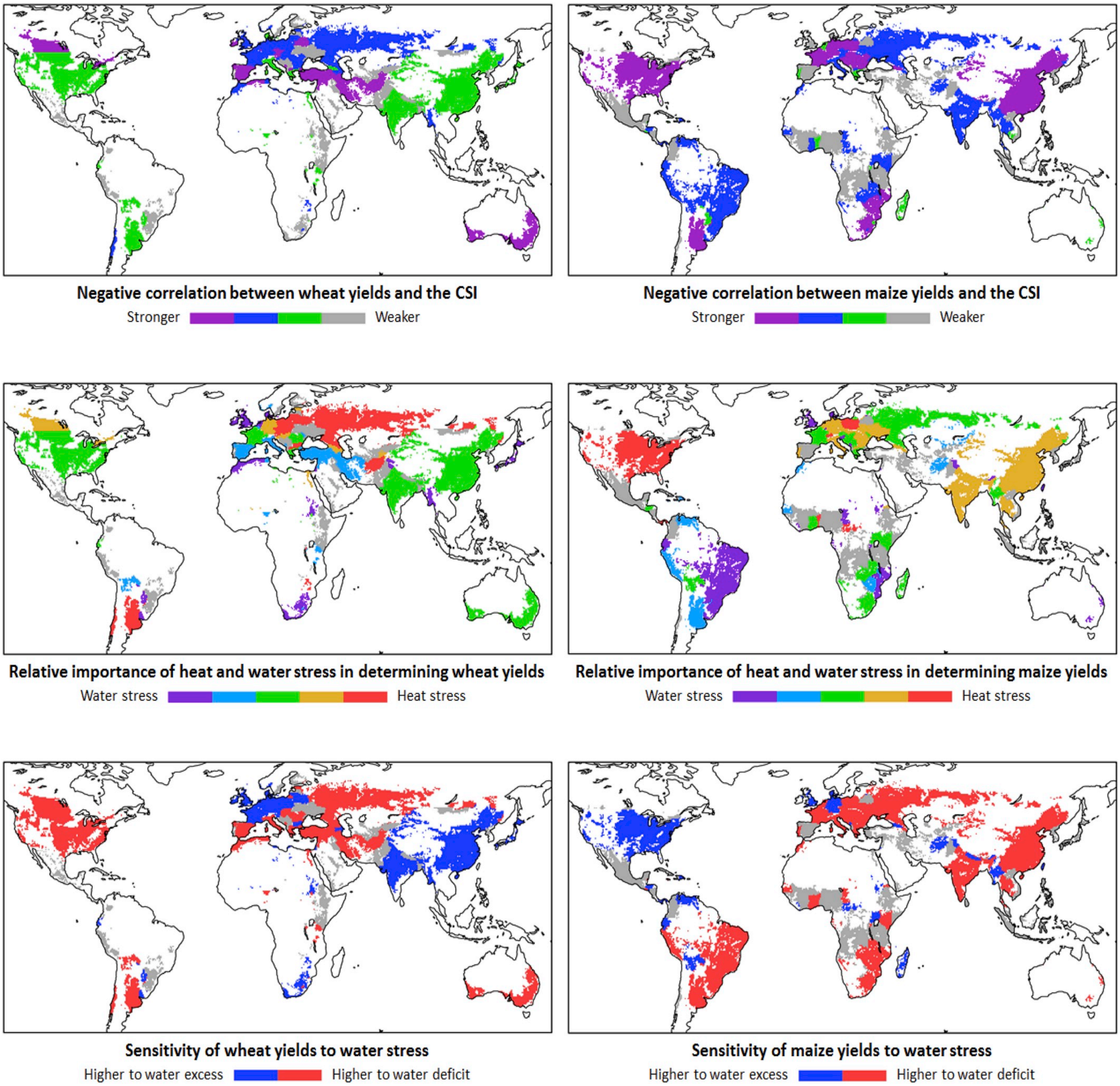

Fig. 1. Variability of crop yields attributed to agroclimatic anomalies.
Note: Top panels show the strength of negative correlation between the Combined Stress Index (CSI) and detrended yields at the country level from 1980 to 2010. Middle panels show the qualitative importance of heat and water stress in determining the CSI. Bottom panels decompose the sensitivity of yields per type of water stress. More details are given in Sections 2.1, 3.1, and Zampieri et al. (2017).
Source: Own elaboration.

that solve as a square system, and represents agricultural and trade policies in detail.[1] Commodity markets clear both at the domestic level, where supply equals demand, and at the world level, where total exports equal total imports. Bilateral trade is not directly inferable as every region trades with the world market as a whole. Data and equations that reflect new country-specific information on agricultural policies are updated annually to facilitate the modelling of potential market developments. Macroeconomic factors such as GDP growth, inflation, exchange rates, oil prices, and population growth enter the system exogenously. These factors remain unchanged in our simulation experiment. More details on the model documentation and Outlook procedure can be found in OECD/FAO (2015) and Araujo-Enciso et al. (2015b).

2.3. Extension of the economic model with the CSI

Crop yields in the standard version of Aglink-Cosimo are modelled endogenously as a linear combination of a time trend, economic drivers, and agricultural policies:

$$ln(YLD)_{r,c,t} = trend + f(PP, SUB, ICS)_{r,c,t} + calib_{r,c,t} \quad (2)$$

[1] In a square system the number of equations equals the number of unknowns.

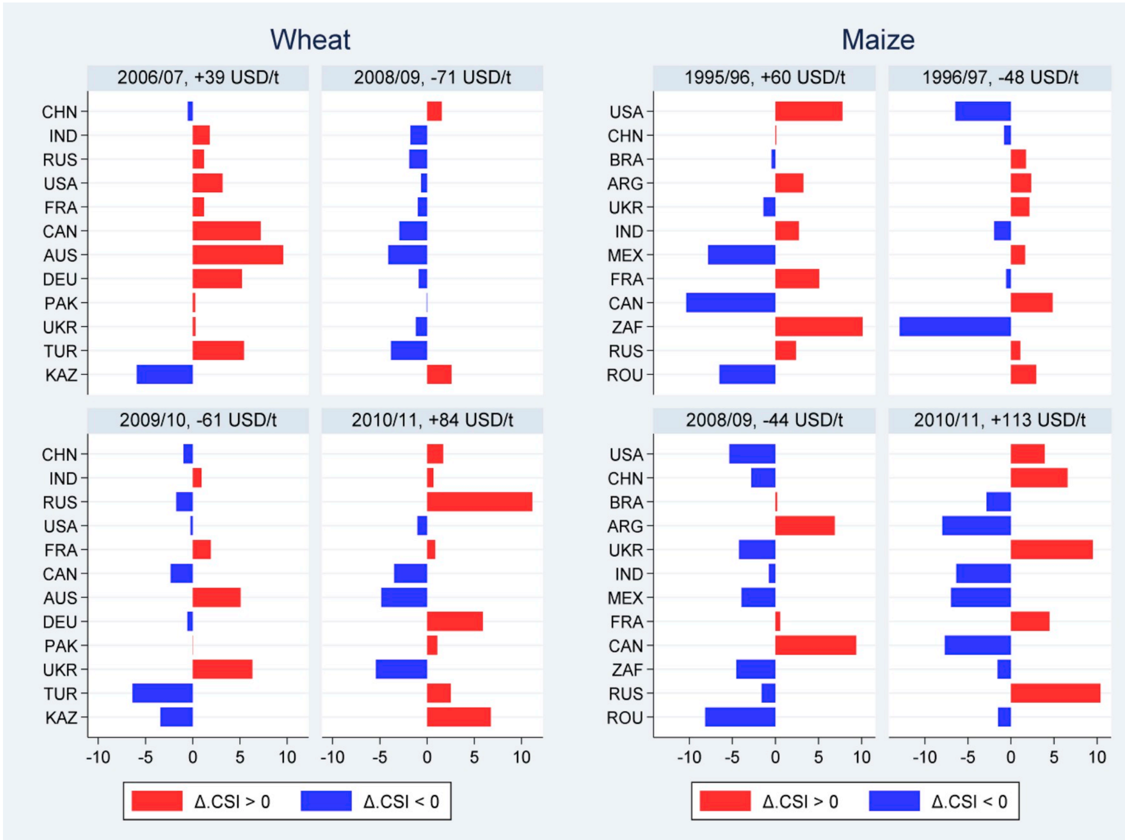

Fig. 2. Concurrent agroclimatic variability and world prices.
Note: Bars show the configuration of country-level agroclimate in years where world prices jumped or dropped the most. Red (blue) denotes deteriorated (improved) crop-growing conditions compared to the previous year, proxied by an increase (decrease) in the value of the Combined Stress Index (CSI; see Section 2.1). Sub-labels show international price changes with respect to the previous marketing year (No. 2, hard red winter wheat, US FOB, Gulf; No. 2, yellow maize, US FOB, Gulf). The Figure highlights: *(i)* the role of geographical compensation (favorable agroclimate leading to food surplus and lower prices in one place often offsets production shortage and higher prices due to unfavorable conditions in another); *(ii)* that concurrent agroclimatic anomalies seem to matter more in the case of wheat, probably due to its geographical spread (the Americas dominate in terms of maize production and exports). The highest correlations between world prices and regional CSI values, all expressed as first-differences, were found for US maize ($r = 0.63, p < 0.01$, 1990–2010) and Russian wheat ($r = 0.41, p < 0.1$, 1990–2010). ISO3 nomenclature. Countries sorted by historical production. (For interpretation of the references to colour in this figure legend, the reader is referred to the Web version of this article.)
Source: Own elaboration based on OECD/FAO (2018).

where *PP* is the producer (farm-gate) price, *SUB* denotes yield- and area-based payments, *ICS* is an index of cost shares, and *r*, *c*, and *t* are region, crop, and year identifiers respectively. The time trend is a proxy for technological change. Expected prices are usually first-order own-lags to parameterize cobweb-like adjustments in crop markets (e.g., that production decisions at *t* are based on prices at *t-1*). The costs index comprises shares of various tradable and non-tradable inputs and is used as a price deflator. Coefficients (e.g., price elasticities) are based on ad hoc empirical estimation, economic theory, and expert knowledge, and remain fixed during simulation. Finally, an intercept and an error serve as interdependent calibration terms as well as 'garbage bins' for omitted or misspecified factors.

The incorporation of the CSI into Aglink-Cosimo was done in three steps. In the first step, the effect of agroclimatic variability on yields was estimated with the nonparametric approach that was used to originally develop the CSI (Zampieri et al., 2017). This led to the estimation of *N* locally weighted scatterplot smoothing (LOWESS) regressions per crop-country combination for the period 1980–2010 (and therefore, $N_{max} = 31$) with a bandwidth of 0.75. The resulting smoothed yields, then, served as dependent variables to estimate the yield-to-CSI coefficients using OLS regression. The attractiveness of the LOWESS approach lies in its locality: it tends to follow the data closely in that extremely high (low) values do not affect the fitting of extremely low (high) values.

In the second step, the matrices resulting from the multiplication of the estimated CSI coefficients (vectors) and the CSI data (matrices) were introduced into Eq. (2) as linearly additive predictors of yields. Finally, the 'new' yield equations were calibrated by adjusting the calibration terms. More specifically, baseline yields (2018 − 2027) in the extended version of the model, where 'normal' agroclimate is parameterized by setting the CSI values equal to zero, are identical to baseline yields from the standard version of the model, where 'normal' agroclimate is assumed without any explicit parameterization. This approach allows for the implementation of exogenous CSI shocks by simply changing the CSI values from zero to non-zero and rerunning the calibrated model. Therefore, the scenario concept turns from the generic *'what if yields dropped'* into the more specific *'what if temperature and/or water stress occurred'*.

2.4. Scenarios

In this study we perform 58 deterministic scenarios of single region-crop-year extremes using the 2018-2027 OECD-FAO baseline (OECD/FAO, 2018). Two mutually exclusive scenarios were examined for 29 crop-region combinations: extremely unfavorable and extremely favorable agroclimate. CSI scenario values were determined on the basis of actual agrometeorological variability over the period 1980–2010: the historical maximum and minimum CSI values per crop and region were

Table 1
Shares (%) in total global production and total global exports, 2013–2017.
Source: Own calculation based on OECD/FAO (2018).

Wheat			Maize			Soybean		
Region	Production	Exports	Region	Production	Exports	Region	Production	Exports
EU-28[M]	21	19	USA	35	38	USA	34	38
China[M]	17	< 1	China[M]	21	< 1	Brazil	31	41
India[M]	13	1	Brazil	8	18	Argentina	17	9
Russian Fed.	9	16	EU-28[M]	6	2	China[M]	4	< 1
USA[M]	8	16	Argentina	3	13	India	3	0
Canada	4	13	Ukraine	3	14			
Australia	4	11	Mexico[M]	2	1			
Pakistan	3	< 1	India	2	1			
Ukraine	3	9	Canada	1	1			
Turkey[M]	3	2	Russian Fed.	1	4			
Kazakhstan	2	5	South Africa	1	1			
Argentina	2	4	E. Europe	1	2			
Sum	88%	95%	*Sum*	86%	94%	*Sum*	89%	88%

Note: 'M' – major importer (absorbed at least 1% of world imports). 'E. Europe' is a regional average of various non-EU countries mainly from the Balkans.

used as shock values, one at a time, in the marketing year 2019/20. 'Normal' agrometeorology –that is, a CSI value of zero – is assumed for the remaining years of the projection horizon. Although we run the model for the whole simulation period, in this article we take a static perspective in the presentation of results and focus on impacts at the year of the shock.

Yield changes are the manifestation of various factors that extend beyond climate. For this reason, contrary to the supply-shock approach, our setup does not assume a yield change of identical magnitude with the historical one; instead, an exogenous CSI shock at year t translates into an endogenous yield response at t based on an empirically established, calibrated, and validated relationship between yields and specific stressors. Eq. (3) shows how the overall impact on crop yields is driven by the direction and size of the CSI shock:

$$CSI_{scen} = \begin{cases} CSI_{max} > CSI_{base} = 0 \rightarrow YLD_{scen} < YLD_{base} \ (damaging \ \ shock) \\ CSI_{min} < CSI_{base} = 0 \rightarrow YLD_{scen} > YLD_{base} \ (beneficial \ \ shock) \end{cases} \tag{3}$$

Extreme events are assumed to hit regions by surprise after planting. The Aglink-Cosimo model does not distinguish between planted and harvested areas, and therefore the resulting yield effect operates as a production effect over the baseline area harvested; in other words, the area effect is zero in the year of the shock. The dynamic structure of the model, however, allows for dynamic –area and other– adjustments beyond the year of the shock. Yield changes at t are transmitted to the system through direct, indirect, own- and cross-crop effects altogether affecting production, consumption, stocks, trade, and prices, which endogenously and dynamically adjust to ensure that markets clear. A simplified description of this transmission mechanism can be found in the Appendix.

2.5. Countries under study

Key wheat, maize, and soybean producers and exporters are listed in Table 1. Most rain-fed (irrigated) wheat production comes from temperate (tropic and sub-tropic) countries, and a large number of regions produce relatively small volumes. The top-12 producers account for 88% of global production, five of which account for three-fourth of world exports. Over half of global maize production comes from the US and the People's Republic of China (henceforth China), the remaining fraction being more dispersed. The US, Brazil, Argentina, and Ukraine account for 83% of global maize exports. Similarly to maize, most soybean production and exports come from the Americas. Consequently, we hypothesize that the extent of sensitivity of the global food system to local extremes depends on the crop and region one may look at. Single events in various countries may affect global wheat prices in rather small amounts, whereas an abrupt change in global maize or soybean prices is more likely to originate from extremes in the US.

3. Results

3.1. Yield response to heat and water stress

The estimated impact coefficients per crop and region are summarized in Table 2 and Fig. 3.[2] Overall, the models show satisfactory explanatory power and the CSI coefficients have the expected negative sign: positive (negative) CSI values are associated with a decrease (increase) in average national yields, ceteris paribus. Among key wheat exporters, yields in Australia, Kazakhstan, Russia, Canada, and some EU conutries show particularly high sensitivity to heat and water stress that exceeds the multi-country mean response. The highest impact coefficients for maize were found for South Africa, Russia, Romania, and Brazil, while US yields are closer to the mean response. The width of the various bars in Fig. 3 represents confidence intervals of the point estimates. It can be seen that the response of yields to compound extremes is more uncertain in some cases, such as wheat in Argentina and maize in Russia. In other cases, the estimated yield response is more precise (e.g., wheat in Turkey, maize in Italy).

A statistically significant effect was not found in two cases for wheat (China and Ukraine) even with alternative model specifications and functional forms. Various reasons are possible for this result. First, overall 'normal' agrometeorology may mask localized extremes. Second, the non-explicit representation of irrigation in the CSI and national yields may confound the response of rain-fed and irrigated areas. Third, the CSI may not capture to the full extent yield effects that are induced by grand-scale agroeconomic practices that lead to persistent yield growth (e.g., intensified fertilization). For these reasons, low sensitivity of wheat yields in China and Ukraine was assumed in the simulation experiment, and CSI coefficients equal to -0.01 were used.

3.2. Domestic wheat markets

Fig. 4 provides an overview of the propagation of extreme events per crop and region to the main elements of the market-clearing equation of the Aglink-Cosimo model: production, consumption, stocks, trade, and prices. Unless mentioned otherwise, results are presented as deviations with respect to the baseline values for the marketing year

[2] More details on the CSI-yield association are given in Zampieri et al. (2017).

Table 2
Sensitivity of crop yields to agroclimatic stress: yield-to-CSI estimates.
Source: Own estimation.

Crop	Region	Coefficient	Std. Er.	R^2	Sample	Method
Wheat	Argentina	−0.0239***	0.0081	23%	1980–2010	LOWESS
	Australia	−0.0541***	0.0058	75%	1980–2010	LOWESS
	Canada	−0.0310***	0.0022	87%	1980–2010	LOWESS
	China	0.0018	0.0026	2%	1982–2010	FD^{AR1}
	EU-15	−0.0110***	0.0037	36%	1993–2010	LOWESS
	EU-N13	−0.0301***	0.0028	89%	1994–2010	LOWESS
	India	−0.0213***	0.0022	81%	1986–2010	LOWESS
	Kazakhstan	−0.0445***	0.0031	92%	1991–2010	LOWESS
	Pakistan	−0.0149***	0.0038	46%	1991–2010	LOWESS
	Russian Fed.	−0.0421***	0.0051	74%	1985–2010	LOWESS
	Turkey	−0.0153***	0.0010	90%	1980–2010	LOWESS
	Ukraine	0.0464	0.0294	32%	1993–2010	FD^{AR1}
	USA	−0.0107**	0.0043	62%	1980–2010	OLS with trend
	Global	−0.0213***	0.0009	42%	1980–2010	LOWESS
Maize	Argentina	−0.0118**	0.0055	87%	1983–2010	OLS with trend
	Brazil	−0.0369***	0.0023	90%	1980–2010	LOWESS
	Canada	−0.0042***	0.0006	64%	1980–2010	LOWESS
	China	−0.0140***	0.0030	43%	1980–2010	LOWESS
	E. Europe	−0.0357***	0.0080	51%	1990–2010	LOWESS
	EU-15	−0.0134***	0.0011	91%	1993–2010	LOWESS
	EU-N13	−0.0460***	0.0014	98%	1994–2010	LOWESS
	India	−0.0102*	0.0052	18%	1991–2010	FD
	Mexico	−0.0203***	0.0024	71%	1980–2010	LOWESS
	Russian Fed.	−0.0520***	0.0089	59%	1985–2010	LOWESS
	South Africa	−0.0715***	0.0063	87%	1990–2010	LOWESS
	Ukraine	−0.0167*	0.0091	16%	1992–2010	FD
	USA	−0.0251***	0.0028	73%	1980–2010	LOWESS
	Global	−0.0200***	0.0006	63%	1980–2010	LOWESS
Soybean	Argentina	−0.0043***	0.0015	21%	1980–2010	LOWESS
	Brazil	−0.0179***	0.0052	29%	1980–2010	LOWESS
	China	−0.0044*	0.0023	14%	1986–2010	LOWESS
	India	−0.0160*	0.0092	35%	1990–2010	OLS with trend
	USA	−0.0129***	0.0013	77%	1980–2010	LOWESS
	Global	−0.0078***	0.0010	20%	1990–2010	LOWESS

Note: Coefficients show the average response of regional yields (t/ha, logarithmized) to a marginal increase in the corresponding Combined Stress Index (CSI). Multiplied by 100, coefficients can be interpreted as semi-elasticities (e.g., a unit increase in the CSI for Australian wheat reduces expected yield by 5.4%). Three estimation methods were used: OLS on smoothed yields generated with locally weighted scatterplot smoothing (LOWESS), first differences (FD), and classic OLS with a linear trend. As wheat yields in China and Ukraine are persistent, the corresponding equations include a first-order autocorrelation term after differencing. Global coefficients are based on pooled estimation (704 yield-CSI pairs from 25 single countries; 602 yield-CSI pairs from 22 single countries; and 263 yield-CSI pairs from 10 non-EU countries, the EU-15 and EU-N13 averages, and E. Europe). All models include an intercept. ***$p < 0.01$, **$p < 0.05$, *$p < 0.1$.

2019/20, which are shown in the Appendix. The following impacts arise from the estimated sensitivity of national yields to extreme events (Section 3.1) and the CSI scenario values, both of which geographically vary.

Under unfavorable agroclimate (amber bar portions in Fig. 4), key wheat-growing regions display yield reductions that range from a staggering −28% (Australia) to −6% (US and Ukraine). Besides Australia, three more regions exceed a reduction of -20%: Canada, Russia, and Kazakhstan. The highest absolute drops, corresponding to −0.9 t/ha and −0.7 t/ha, were found in Canada and Russia. Yield losses translate into proportional production cutbacks, the most marked of which are found in Russia (−19 million t), the EU (−11 million t), India and China (−10 million t), Canada (−8 million t), and Australia (−7 million t). In the remaining cases production falls by less than 4 million t. Lower supply leads domestic markets to clear at higher producer prices both in key exporters (16% in Russia, 11% in Kazakhstan, 8% in the EU) and large importing countries such as India (36%). Positive cross effects lead to higher prices of low-protein feed (substitutes), such as coarse grains, cereal brans, dried beet pulp, molasses, beet roots and tuber, across all cases. Taking all types of protein feed and cross-price effects into account, feed prices rise the most in Russia, Kazakhstan, Pakistan, and India (up to 7%). Due to the higher cross-price elasticities, consumer prices increase by up to one third, most notably in Asian countries.

The potential impacts of negative extremes are more pronounced on trade. With respect to the baseline, export volumes drop dramatically in Russia (−15 million t), Australia, the EU, and Canada (−7 million t in each). Furthermore, all-time-low stock-to-use ratios can be noted for Pakistan (0.04) and Canada (0.5), while Turkey displays record-low self-sufficiency (0.83) and record-high import-dependency (0.29).[3,4,5] The latter two ratios are close to their historical minima also in the Australian, Chinese, and Indian scenarios, while Pakistan turns into a net importer for one year. In the EU scenario, ad-valorem tariffs currently levied on various imported grains decrease by a maximum of three percentage points in order for domestic (feed) demand to be met with higher non-wheat imports. At the global level, the culmination of lower availability of wheat leads 2019/20 international prices to rise across scenarios, most pronouncedly in the case of extreme events in Russia (10%; +20 USD/t) , the EU (5%; +11 USD/t), Australia or Canada (4%; +8 USD/t).[6]

The picture is reversed if extremely favorable agroclimate is assumed, where yield increases up to 41% are observed (Kazakhstan case;

[3] *Stock-to-use ratio = ending stocks ÷ consumption.*
[4] *Self-sufficiency ratio = production ÷ (production + imports – exports).*
[5] *Import-dependency ratio = imports ÷ (production + imports – exports).*
[6] No. 2, hard red winter wheat, US FOB, Gulf.

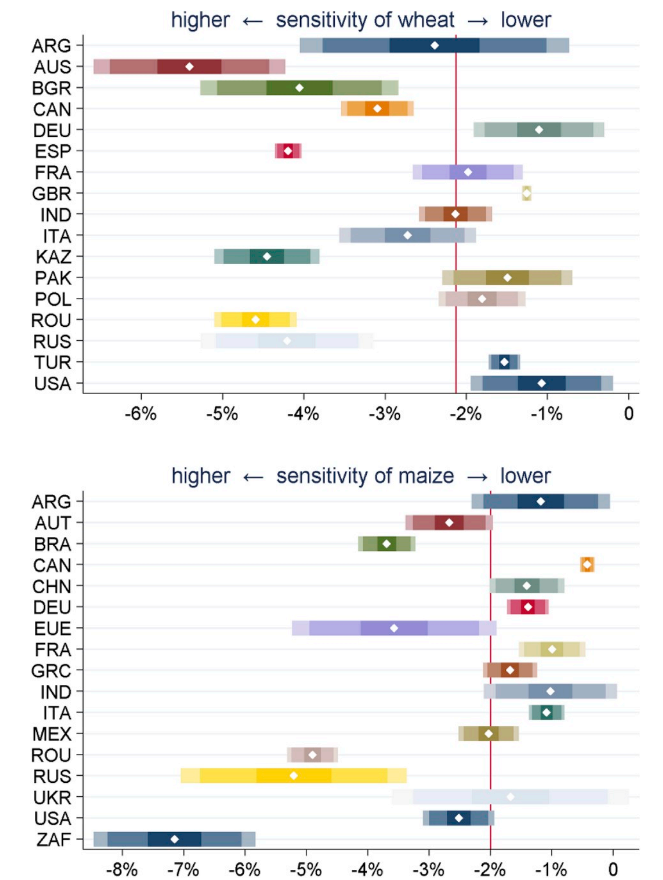

Fig. 3. Sensitivity of crop yields to agroclimatic stress in selected regions, 1980-2010.
Note: Coefficients (dots within bars) show the average relative response of regional yields to a marginal increase in the corresponding Combined Stress Index (CSI). Bar shades represent 50%, 90%, and 95% confidence intervals around the point estimates. Red lines show the multi-country mean response from two pooled models. More details are given in Sections 2.1, 3.1, and Table 2. ISO3 nomenclature (EUE – aggregate for E. Europe). (For interpretation of the references to colour in this figure legend, the reader is referred to the Web version of this article.)
Source: Own estimation based on OECD/FAO (2018) and Eurostat (2017).

green bar portions in Fig. 4). The larger absolute jumps relative to the baseline correspond to Australia and Argentina (+0.7 t/ha), Canada (+0.6 t/ha), and Russia and Kazakhstan (+0.5 t/ha). Salient production expansions can be noted in Russia (+14 million t), Australia and China (+9 million t each), the EU (+8 million t), and Canada and Kazakhstan (+6 million t each). Regional overproduction leads to a drop in domestic producer prices particularly in Pakistan (-13%) and Kazakhstan (−10%) but also in India, Russia, and Australia (between −9% and −6%). Lower prices induce an increase in low-protein feed use while average feed prices drop by 6% (case of Kazakhstan) or less. Following an excess supply of wheat, consumer prices decline the most in Pakistan (−6%), India and China (−4% each).

Wheat exports rise by a staggering 11 million t in Russia, 9 million t in Australia, and between 6 and 4 million t in Kazakhstan, the EU, and Canada. Record-high self-sufficiency ratios can be noted for the EU-28 (1.24) and Russia (2.1), while Turkey becomes a net exporter of wheat for one year. Higher global wheat availability and improved trade balances throughout reduce international prices by 6% (-12 USD/t; Russian shock), 4% (Australian case), 3% (EU and Kazakhstan cases), or less.

3.3. Domestic maize markets

Key maize-growing regions display yield reductions that range from −49% (South Africa) to a mere −3% (Canada) (Fig. 5). Sharp absolute drops are detected for South Africa (−2.8 t/ha), the US (−2.5 t/ha), Russia (−1.6 t/ha), and the EU (-1.4 t/ha). These are the result of sizeable production losses, mainly in the US (−82 million t; −22%) but also in other key regions such as China (−23 million t), the EU (−13 million t), Brazil (−10 million t), and South Africa (−7 million t). Domestic producer prices build up the most in the latter country (> 300%) as well as India (52%) and the US (44%). As a result, feed prices double in South Africa and increase by one-fourth in the US, while consumer prices surge in South Africa (one-third) and China (one-fourth).

Unfavorable conditions for maize lead to a substantial decrease in US export volumes with respect to the base (−38 million t) with the effect ranging from −8 (Brazil) to −3 million t (Ukraine) among the next three exporters. On the other hand, maize imports roughly double in the EU (+10 million t) following an endogenous decrease in the import tariffs on various grains, while they also rise by about 2 million t in Mexico (16%) and China (43%). India and South Africa become net importers for one year, and record-low self-sufficiency (Argentina, China, EU, USA) and record-high import-dependency ratios (China, EU, Mexico) are marked in a number of cases. The strongest transmission on the world market price comes from the US (35%; +57 USD/t), which makes up the lion's market share in global exports; impacts in the remaining shocks do not exceed the level of 5% (+8 USD/t; EU case, corresponding to surged import demand).[7]

Extremely favorable agrometeorology reverses the yield picture especially in South Africa (+3.2 t/ha), Eastern Europe (+1.6 t/ha), the EU (+1.5 t/ha), and the US (+1.4 t/ha). In some cases, boosted yields lead to record production. For example, simulated US yields of 12.5 t/ha lead to the production of 414 million t thus surpassing the previous historical record (2016/17). Similarly, production in Brazil and Argentina climb to 101 and 44 million t against historical records of 99 (2017/18) and 40 (2016/17) million t respectively. Producer prices drop the most in South Africa (−21%), the US, China, and the EU (−14% each), while lower changes are observed in the remaining regions. Average protein feed prices decline between −10% and −5% in most cases and low-protein feed gains importance across all scenarios. Consumer prices fall mainly in China (−14%) and South Africa (−5%). Exports expand notably in the US scenario (+18 million t) but also in South Africa (+9 million t), Brazil (+8 million t), and Ukraine and Argentina (+4 million t each). Given higher domestic supplies, maize imports drop by one-third in Mexico (−4 million t), about half in China (−2.5 million t), and two-thirds in the EU (−7 million t), where import tariffs rise by up to two percentage points. The international price of maize falls by 13% (−21 USD/t) due to the US shock and by a lower amount in the remaining cases (e.g., −7 USD/t in the Brazilian scenario).

3.4. Domestic soybean markets

Fig. 6 depicts potential market effects from agroclimatic extremes in key soybean regions. The largest productions cutbacks are found in the US (−14 million t), Brazil (−7 million t), and Argentina (−2 million t). Domestic producer prices build up the most in India (58%), the US (16%), and Brazil (10%), while a substitution of more expensive higher-protein meals with cheaper medium- and low-protein meals is observed across scenarios. US and Brazilian exports decrease substantially with respect to the baseline by about 10 million t (−17%) and −6 million t (9%) respectively. The opposite effects are obtained in the case of extremely favorable crop-growing conditions. Depending on the scenario, the international price of maize is impacted the most in the US

[7] No. 2, yellow maize, US FOB, Gulf.

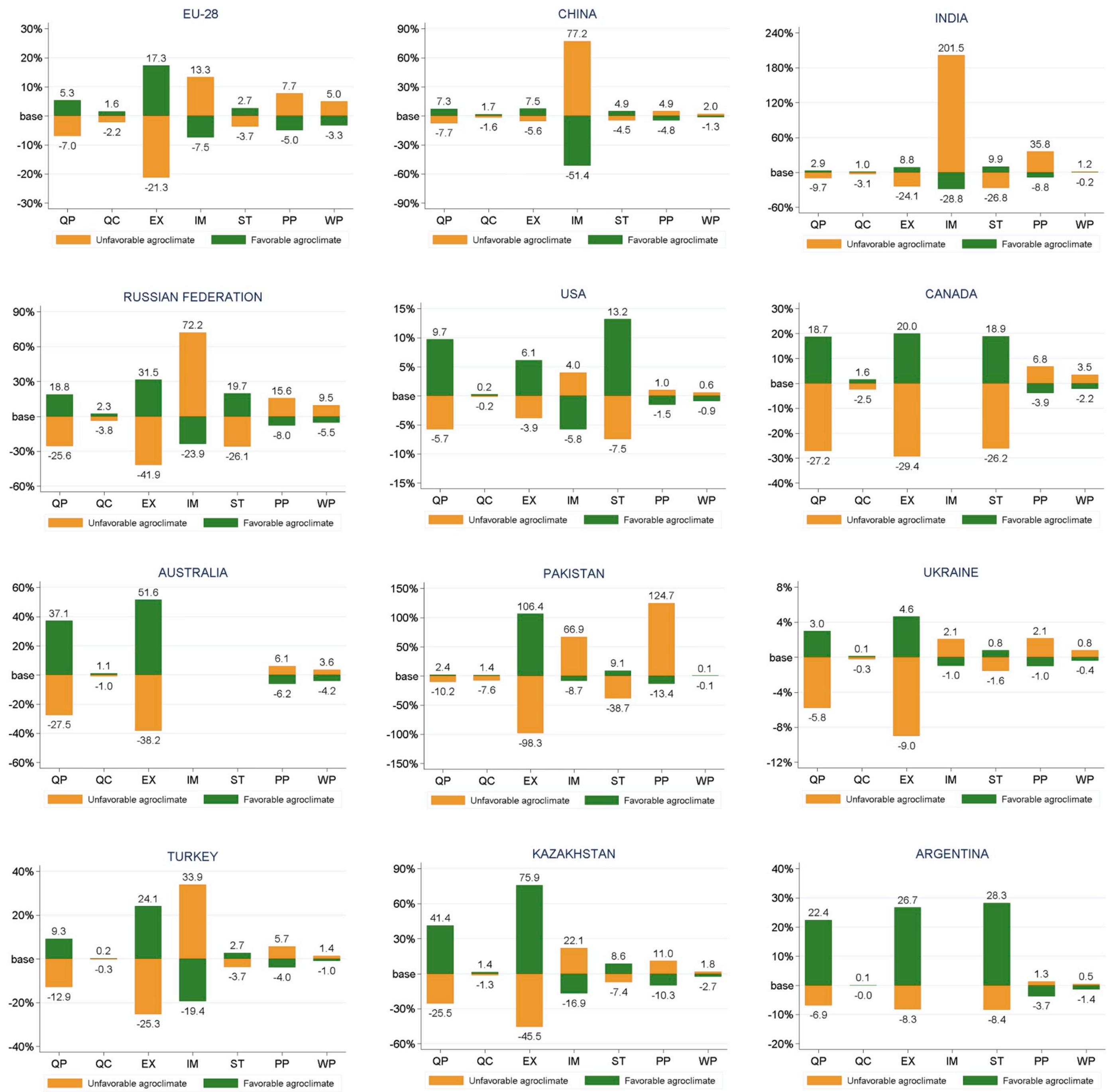

Fig. 4. Simulated agroclimatic extremes and domestic wheat markets, 2019/20.
Note: Each panel shows the potential impact of extreme temperature and water anomalies under single region-crop-year scenarios. Bars show % deviation from the baseline levels that can be found in the Appendix. 'QP' – production, 'QC' – consumption (all uses), 'EX' – exports, 'IM' – imports, 'ST' – ending stocks, 'PP' – producer price, 'WP' – world price (No. 2, hard red winter wheat, US FOB, Gulf). (For interpretation of the references to colour in this figure legend, the reader is referred to the Web version of this article.)
Source: Own estimation based on OECD/FAO (2018).

(± 15%; ± 61 USD/t) and Brazilian (± 9%; ± 36 USD/t) cases.[8]

3.5. The global picture

Temporary production shortages (surpluses) are responsible for lower (higher) stocks that eventually resume to their equilibrium. Fig. 7 shows that extremes in key regions are visible on global market fundamentals at the year of the shock, thus confirming the expected inverse relationship between global stock utilization and international crop prices.

In the case of wheat, the response of global stock-to-use ratios and prices stands out in the case of Russia. This is attributed to a relatively high average sensitivity to extremes, high CSI shock values, and large export volumes that are expected to surpass the respective EU volumes. The impacts of extreme agrometeorology in Australia, Canada and other countries are also globally noticeable. For maize and soybean, the

[8] US soybean, CIF Rotterdam.

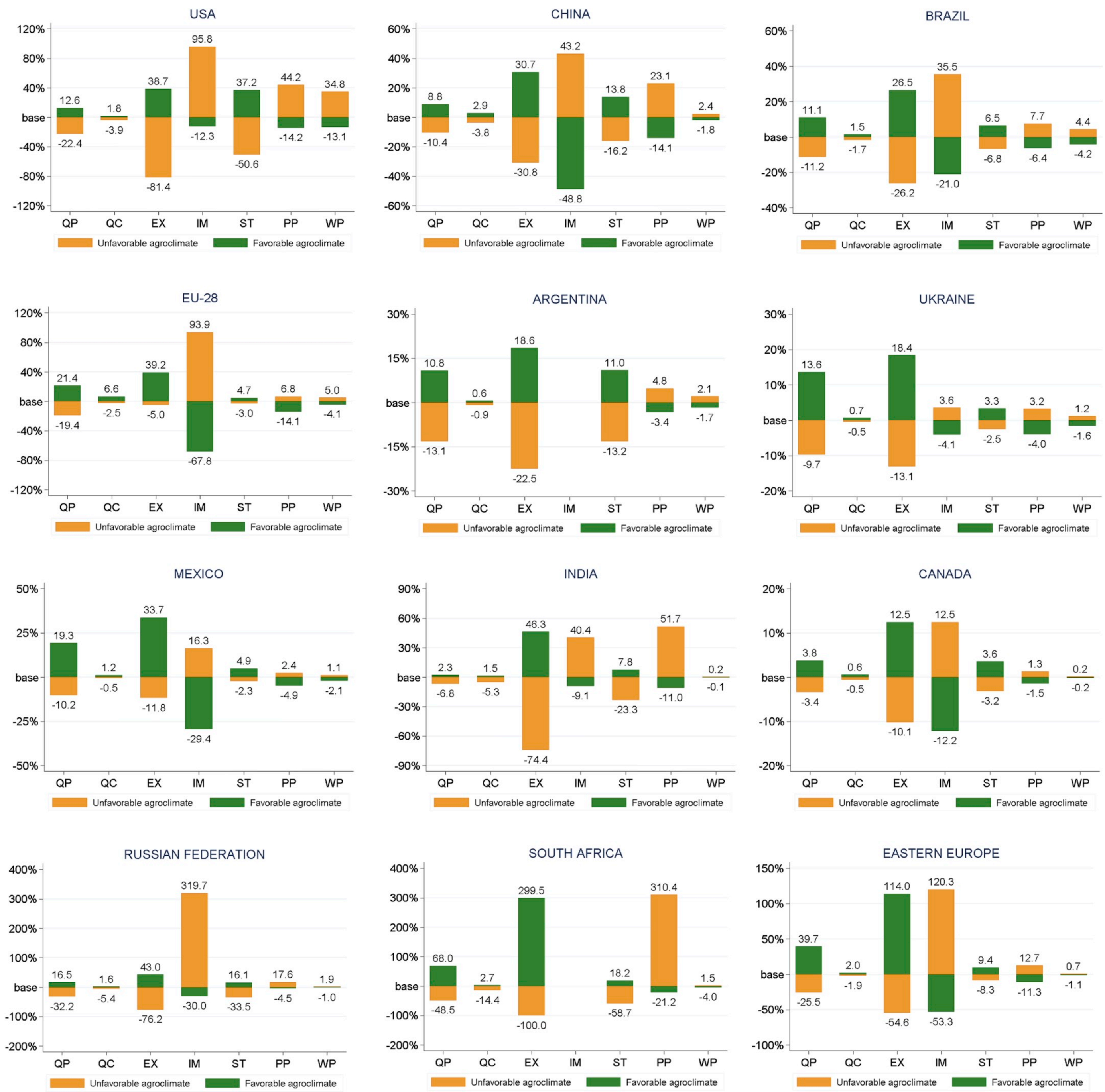

Fig. 5. Simulated agroclimatic extremes and domestic maize markets, 2019/20.
Note: Each panel shows the potential impact of extreme temperature and water anomalies under single region-crop-year scenarios. Bars show % deviation from the baseline levels that can be found in the Appendix. 'QP' – production, 'QC' – consumption (all uses), 'EX' – exports, 'IM' – imports, 'ST' – ending stocks, 'PP' – producer price, 'WP' – world price (No. 2, yellow maize, US FOB, Gulf). (For interpretation of the references to colour in this figure legend, the reader is referred to the Web version of this article.)
Source: Own estimation based on OECD/FAO (2018).

US stands out due to high shock values that correspond to past El Niño and la Niña years, as well as due to high market shares.

An interesting pattern is noticeable in the sense that endogenously determined global stock-to-use ratios and prices occasionally diverge from a rather symmetric line on which most countries virtually lie. Those cases point presumably to nonlinearities in the response of global market fundamentals that may be attributed to heterogeneous domestic and trade policies that are currently in place to ensure international competitiveness or to achieve or maintain self-sufficiency. Two examples included into Aglink-Cosimo pertain to the emergency/humanitarian and food security stockpiles for wheat in China and India as well as the Agricultural Risk Coverage and Price Loss Coverage programs in the US.

4. Discussion and conclusions

Agroclimatic extremes constitute a substantially under-researched area both in terms of attribution, likelihood, magnitude of potential

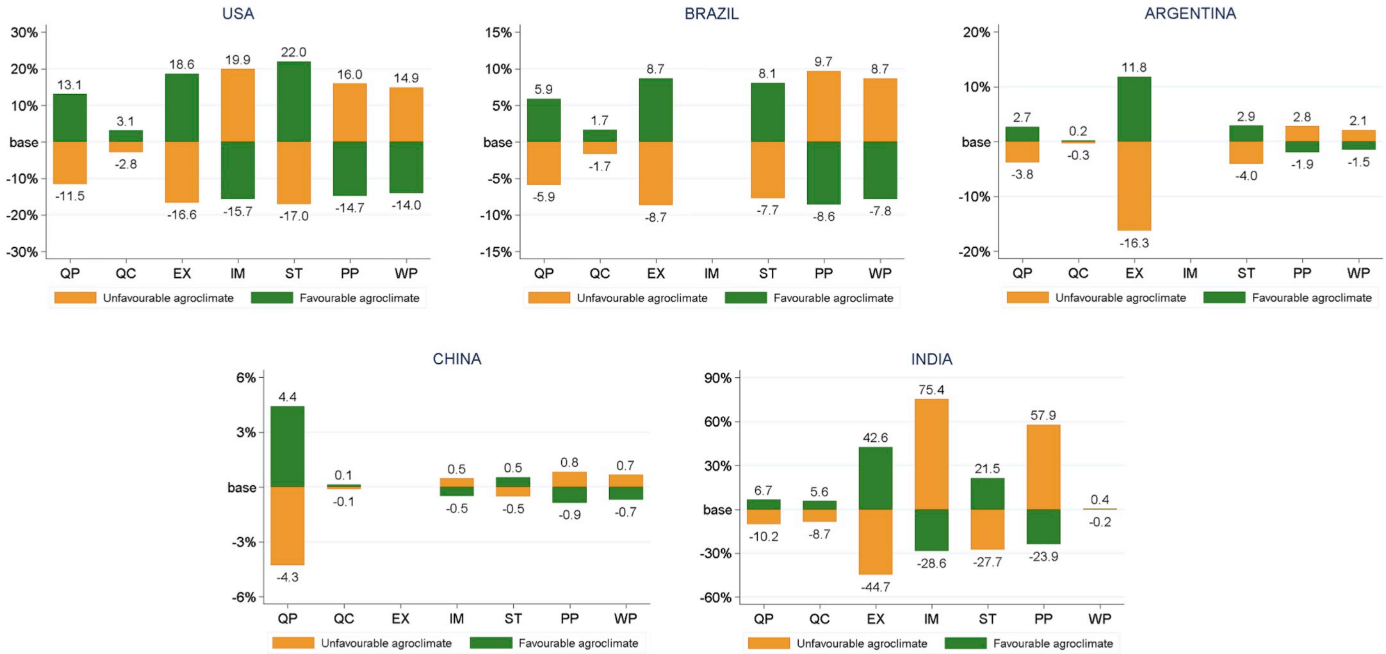

Fig. 6. Simulated agroclimatic extremes and domestic soybean markets, 2019/20.
Note: Each panel shows the potential impact of extreme temperature and water anomalies under single region-crop-year scenarios. Bars show % deviation from the baseline levels that can be found in the Appendix. 'QP' – production, 'QC' – consumption (all uses), 'EX' – exports, 'IM' – imports, 'ST' – ending stocks, 'PP' – producer price, 'WP' – world price (US soybean, CIF Rotterdam).
Source: Own estimation based on OECD/FAO (2018).

impacts, and crops and regions covered, let alone bringing these aspects together in the form of integrated assessment. In this article we contributed to the empirical literature by incorporating a compound yield stress index into a partial equilibrium model of global agriculture. By re-enforcing extreme climatic conditions of the past into the near future we simulated the corresponding potential short-to-medium term impacts on key domestic and international commodity markets.

Agroclimatic extremes can be seen as typical supply shifters that temporarily alter crop availability and distort commodity markets. The response of prices is in conceptual accordance with expectations: depending on the direction of the shock, extreme agroclimatic anomalies lead crop prices to clear significantly above or below the baseline projections, which typically assume 'normal' agroclimate without modelling it. At the domestic level, the magnitude of the price response differs per crop-country combination and depends mainly on the local sensitivity of food systems to extremes (i.e., the CSI coefficients) and the market status-quo at the time of the shock. The transmission of domestic prices to global markets is visible in most scenarios with large shocks in key exporters and importers being responsible for the most pronounced effects.

A particularly interesting finding is that the endogenously transmitted effect on commodity prices is asymmetric. In the vast majority of cases, domestic and world prices appear to be more responsive to negative agrometeorological anomalies rather than to positive ones (e.g., see Australian panel in Fig. 4 where price effects of similar relative magnitude result from yield changes of different size). This implies that abundant grain supplies (i.e., high inventories, like those of the last five years) and trade exert downward pressure on prices that may not always be enough to ameliorate the damage from extreme events. The challenge lying ahead is that persistent large-scale harvest failures may deplete grain stocks and thus render future prices even more responsive. A number of creative ways to help mitigate potential food crises have been suggested such as rethinking of international trade regimes and the formalization of grain reserve arrangements (Headey and Fan, 2010). However, the exploration of the potential role of strategic international response, be it within the World Trade Organization's reform programs or in the form of multi-country emergency reserves, requires a deeper understanding of the attributes of concurrent and recurrent shocks across the globe. Too uncertain extremes will render difficult the specification of optimal stock quantities to be held and agreed upon, and governments may be trapped in risk-averse or risk-taking behavior (Lassa et al., 2018). Furthermore, buffer stock schemes for stabilizing supply and prices of major staple commodities in food-insecure regions may mitigate some of the induced price volatility but are generally difficult to achieve and sustain in practice (Thompson et al., 2012).

In terms of trade, negative agroclimatic anomalies translate into a negative domestic supply shock that ultimately dictates lower domestic export demand and higher import demand. The reverse applies for positive agroclimatic anomalies. We find significant trade impacts in either direction indicating both winners and losers, depending on the direction of the shock. Developed countries may lose or gain market shares, while developing economies may face temporary self-sufficiency issues and domestic price destabilization. In this respect, national agencies should investigate the main mechanisms of food price transmission from other regions through trade and elaborate policies to protect the local smallholder farming communities (Arias et al., 2013).

In interpreting our results some important remarks ought to be made. First, the most extreme agroclimatic anomalies of the recent past were taken as scenario values in the simulation experiment. This is attributed to the recent development of the CSI, and hence the absence of CSI projections at the time of this analysis. Second, the correlation of extreme events across crops and countries merits further examination. Third, only single-year events were examined. The dynamic impacts of such events are moderated by a return to average growing conditions next year and, by definition in our experiment, by the absence of simultaneous extremes in other countries. Extremes may recur and commodity prices, as well as other elements of the economic system (e.g., area allocation, trade), would not settle immediately to their long-run equilibrium; in fact, they would under- or over-shoot it following cobweb-like adjustments before fluctuations theoretically decayed (Norwood and Lusk, 2008, p. 131). Further inspection of the dynamic results, which we leave for future investigation, showed that some shocks may indeed be extreme enough to destabilize prices over the

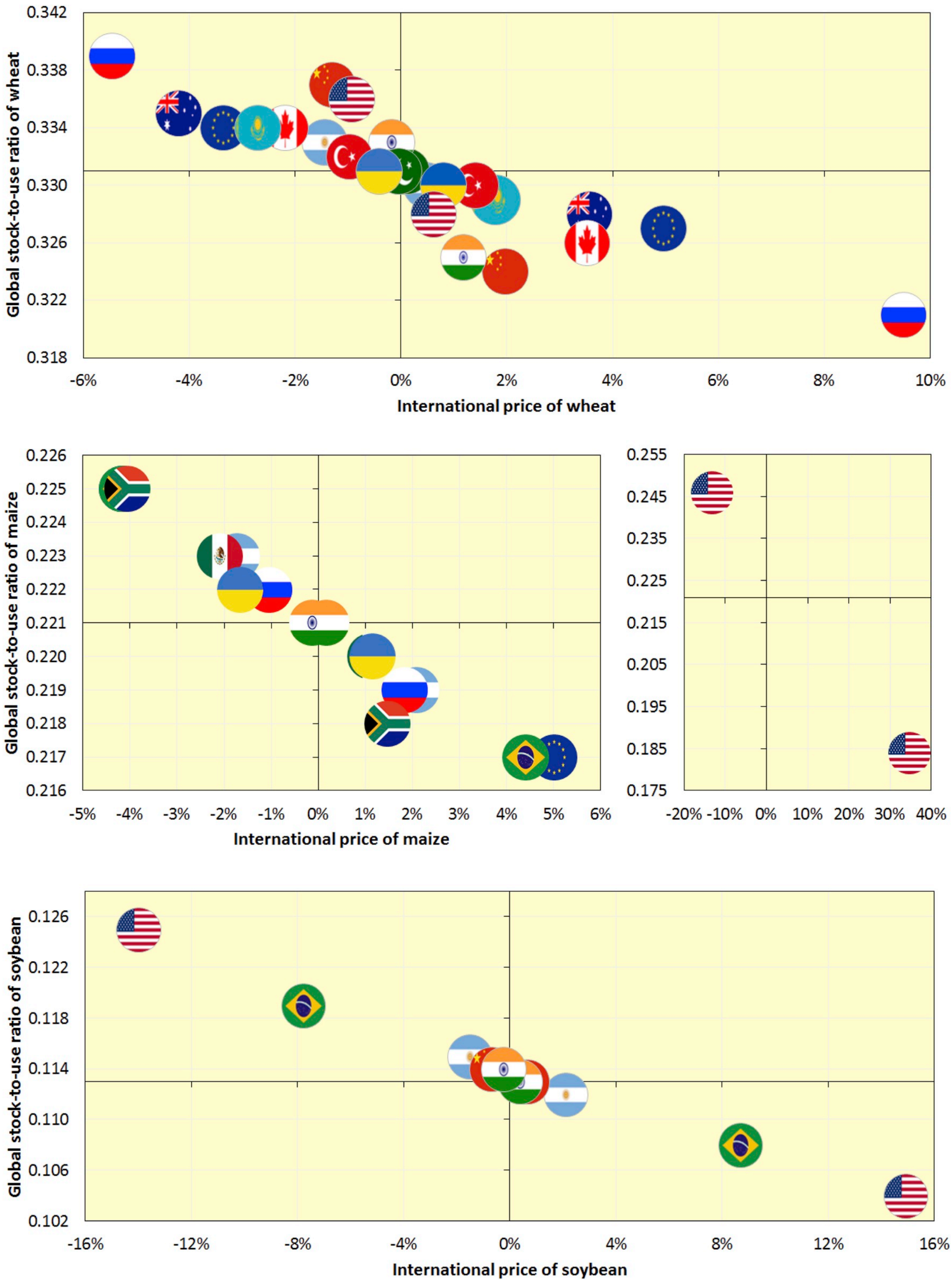

Fig. 7. Simulated agroclimatic extremes and international crop markets, 2019/20.
Note: Bubbles show how regional extreme events may affect global markets (e.g., extremely unfavorable conditions for wheat production in Russia would lead the world price to rise by about 10% and the global stock-to-use ratio to drop to about 0.320). Price references are No. 2, hard red winter wheat, US FOB, Gulf; No. 2, yellow maize, US FOB, Gulf; and US soybean, CIF Rotterdam. Baseline levels can be found in the Appendix. (For interpretation of the references to colour in this figure legend, the reader is referred to the Web version of this article.)
Source: Own estimation based on OECD/FAO (2018).

whole projection horizon. Finally, the supply side of Aglink-Cosimo does not distinguish between rain-fed and irrigated farming activities. Although this may not pose a significant issue for the generation of medium-term market projections, slow changes in the adaptive capacity of each region may alter the long-term picture. Overall, without projections of extreme events little can be said about the degree of future exposure and vulnerability to extremes, which will likely be shaped by evolving adaptation potential in the form of early warning systems, changing water availability and efficiency of use, and increasing adoption of heat-resistant crop varieties. Therefore, although our analysis provides the first global picture of potential effects from regional extreme events, it only paves the way for more advanced analyses to be conducted.

Moving beyond the implementation of deterministic scenarios a promising avenue is the consideration of uncertainty in the attributes of extreme events. In order to understand the potential paths of commodity markets due to stochastic agroclimatic anomalies, we are currently developing a methodological framework that takes into account data and parameter uncertainty. Data uncertainty refers to the generation of stochastic extreme events that reflect globally concurrent and recurrent anomalies up to the year 2030, while parameter uncertainty pertains to potentially evolving sensitivity of yields to extremes. Ultimately, we hope to elaborate on the quantification of risk (magnitude × probability) of extreme events which is a requirement to investigating case-specific policy mechanisms that may ameliorate devastating economic and social consequences on the agricultural sector.

Conflicts of interest

The authors declare no conflict of interest.

Data availability

The Aglink-Cosimo model documentation can be found in OECD/FAO (2015) and Araujo-Enciso et al. (2015b). The agricultural baseline projections used in this article are freely available at http://www.agri-outlook.org/. All data are available from the authors upon request.

Disclaimer

The views expressed are purely those of the authors and may not in any circumstances be regarded as stating an official position of the European Commission.

Acknowledgement

We thank three anonymous reviewers for providing constructive feedback on an earlier version of the manuscript. We are grateful to Lisa Alexander (Editor-in-Chief) and Selvaraju Ramasamy (Associate Editor) for coordinating the review process and offering us the opportunity to include this study into the special issue 'Managing risks of weather and climate extremes: Building resilient livelihoods for food security and nutrition'. The work underlying this article has been funded under the in-house project C^{2}ESAM (‘Concurrent Climate Extremes and Shocks on Agricultural Markets’), for the initial conceptualization of which we would also like to thank our colleague Fabien Santini. Publication costs were covered by the FAO.

Appendix

Table A1
Baseline projections for domestic markets, 2019/20.

Crop/Region	YLD	QP	QC	EX	IM	ST	PP
Wheat							
EU-28	5.83	155.3	129.1	31.7	5.4	13.9	167
China	5.33	127.5	131.1	0.2	3.8	104.8	2138
India	3.16	101.1	100.7	0.4	1.0	17.0	15,686
Russia	2.71	75.2	41.8	35.7	0.3	9.6	8553
USA	3.21	50.8	31.1	25.1	3.6	23.7	172
Canada	3.24	30.0	8.4	22.2	0.1	5.5	189
Ukraine	4.25	27.6	10.4	17.3	< 0.1	1.2	5585
Pakistan	2.92	27.1	26.9	0.1	< 0.1	1.6	22,727
Australia	1.98	25.0	7.2	17.8	< 0.1	5.9	259
Turkey	2.91	22.4	23.3	4.2	5.1	1.0	921
Argentina	3.08	17.1	6.0	11.2	< 0.1	3.0	2850
Kazakhstan	1.24	14.7	7.1	7.5	0.1	3.1	61,909
Maize							
USA	11.08	368.2	326.0	47.2	1.3	59.0	142
China	6.14	225.4	232.0	< 0.1	5.0	77.7	2206
Brazil	5.50	91.2	62.6	31.0	0.7	11.4	524
EU-28	7.23	64.8	73.2	2.5	10.8	16.7	174
Argentina	7.45	39.5	19.4	20.0	< 0.1	3.9	2892
India	2.83	27.4	27.1	0.3	0.1	0.9	11,487
Ukraine	5.89	27.2	7.7	19.5	< 0.1	2.1	4264
Mexico	3.47	26.0	39.8	0.7	13.7	5.2	4124
S. Africa	5.14	14.8	12.0	3.0	0.0	4.1	2010
Russia	4.83	14.5	9.6	4.9	0.1	0.7	7934
Canada	9.88	14.3	13.8	1.7	1.2	2.7	173
E. Europe	4.45	8.0	6.4	2.0	0.2	6.1	143
Soybean							
USA	3.28	118.7	60.2	59.9	0.7	11.0	357
Brazil	3.21	116.5	50.5	66.5	0.4	3.0	1416
Argentina	3.15	56.9	45.7	11.3	< 0.1	4.0	4988
China	1.96	16.6	116.3	0.2	100.1	15.0	4176
Canada	2.87	8.5	2.7	6.1	0.3	0.4	436

Note: ‘YLD’ – yield (t/ha), ‘QP’ – production (million t), ‘QC’ – consumption (all uses; million t), ‘EX’ – exports (million t), ‘IM’ – imports (million t), ‘ST’ – ending stocks (million t), ‘PP’ – producer price (domestic currency/t; USD/t for E. Europe). Regions sorted by projected production.
Source: OECD/FAO (2018).

Table A2
Baseline projections for international markets, 2019/20.

Crop	World price, USD/t	World stock-to-use ratio
Wheat	214	0.331
Maize	163	0.221
Soybean	409	0.113

Note: Price references are No. 2, hard red winter wheat, US FOB, Gulf; No. 2, yellow maize, US FOB, Gulf; and US soybean, CIF Rotterdam.
Source: OECD/FAO (2018).

Table A3
Main model equations (simplified).

Domestic markets	
Clearing:	*Producer Price s.t. Domestic Supply = Domestic Demand,* or equivalently
	Production - Consumption + Imports - Exports + Beginning Stocks - Ending Stocks = 0
Supply:	*Production = Yield x Area Harvested*
	Yield = trend + f (expected prices deflated by costs, subsidies) + calib
	Area Harvested = f (production incentives and relative returns of the given crop relative to other annual crops) + calib
Demand:	*Consumption = Food Use + Feed Use + Other Uses* (e.g., *Crushing, Biofuel)*
	Food Use = f (consumer prices, Consumer Price Index, GDPI, population) + calib
	Feed Use = f (meat and milk production, feed prices) + calib
	Consumer Price = f (GDPD, producer price) + calib
	Feed Prices = f (crop prices categorized by protein content and feed use)
Stocks:	*Ending Stocks = f (lagged stocks, production, disappearance, lagged producer prices) + calib*
	Beginning Stocks = last year's Ending Stocks
Trade:	*Exports = f (relative competitiveness of domestic prices to world prices, exchange rates, domestic policies such as export tariffs) + calib*
	Imports = f (relative competitiveness of domestic prices to world prices, exchange rates, domestic policies such as import tariffs) + calib
World markets	
Clearing:	*World Price s.t. Total Exports = Total Imports + SD,* where
	SD is the 'statistical difference' correcting for data discrepancies that stem from unbalanced trade statistics.

Note: Region, crop, and year subscripts dropped for simplification. The model is described in detail in OECD/FAO (2015) and Araujo-Enciso et al. (2015b).

Table A4
How the CSI shock works.

Following the procedure described in Section 2, an exogenous CSI shock at year *t* leads to:

- A direct change in yields at *t* and an equiproportional change in production at *t*;
- An indirect change on the other elements of the domestic clearing equation (i.e., consumption, trade, ending stocks) at *t*;
- A new producer price at *t* induced by all the above changes, and a new world price at *t* that results from all regional crop supplies;
- A temporal transmission of the above effects through lags to next years (to reflect dynamic market adjustment) till the impacts attenuated and markets returned (close) to the baseline.

References

Araujo-Enciso, S.R., Pérez Dominguez, I., Santini, F., 2015a. Implications of extreme weather events on global agriculture: the El Niño Southern Oscillation event. In: Paper presented at the 10th AEEA Congress (Congresso de la Asociación Española de Economía Agraria), Córdoba, 9-11 September.

Araujo-Enciso, S.R., I. Pérez Dominguez, I., Santini, F., Hélaine, S., 2015b. Documentation of the European Comission's EU Module of the Aglink-Cosimo Modelling System. JRC Science and Policy Report, pp. JRC92618.

Araujo-Enciso, S.R., Fellmann, T., Santini, F., M'barek, R., 2017. Eurasian grain markets in an uncertain world: a focus on yield variability and harvest failures in Russia, Ukraine and Kazakhstan and their impact on global food security. In: Gomez y Paloma, S., Mary, S., Langrell, S., Ciaian, P. (Eds.), The Eurasian Wheat Belt and Food Security. Springer, Cham, pp. 247–257.

Arias, P., Hallam, D., Krivonos, E., Morrison, J., 2013. Smallholder Integration in Changing Food Markets. Food and Agriculture Organization of the United Nations.

Baffes, J., Haniotis, T., 2010. "Placing the 2006/08 Commodity Price Boom into Perspective." Policy Research Working Paper 5371. The World Bank.

Bailey, R., Benton, T.G., Challinor, A., Elliott, J., Gustafson, D., Hiller, B., Jones, A., Jahn, M., Kent, C., Lewis, K., Meacham, T., Rivington, M., Robson, D., Tiffin, R., Wuebbles, D.J., 2015. Extreme Weather and Resilience of the Global Food System. Final Project Report from the UK-US Taskforce on Extreme Weather and Global Food System Resilience. The Global Food Security Programme, Swindon, UK.

Chinese Ministry of Agriculture, 2016. China Agricultural Outlook 2016-2025. Market Early Warning Expert Committee, pp. 159p.

European Commission, 2017. EU Agricultural Outlook for the Agricultural Markets and Income, 2017-2030. DG Agriculture and Rural Development, Brussels.

Eurostat, 2017. Crop statistics database. http://ec.europa.eu/eurostat/data/database.

Fuss, S., Havlik, P., Szolgayova, J., Schmid, E., Heinrich Reuter, W., Khabarov, N., Obersteiner, M., Ermoliev, Y., Ermolieva, T., Kraxner, F., 2015. Global food security & adaptation under crop yield volatility. Technol. Forecast. Soc. Change 98.

Headey, D.,D., Fan, S., 2010. Reflections on the Global Food Crisis: How Did it Happen? How Has it Hurt? and How Can We Prevent the Next One? International Food Policy Research Institute, Washington, DC.

IPCC, 2012. In: Barros, C.B.V., Stocker, T.F., Qin, D., Dokken, D.J., Ebi, K.L., Mastrandrea, M.D., Mach, K.J., Plattner, G.-K., Allen, S.K., Tignor, M., Midgley, P.M. (Eds.), Managing the Risks of Extreme Events and Disasters to Advance Climate Change Adaptation. A Special Report of Working Groups I and II of the Intergovernmental Panel on Climate Change. Cambridge University Press, Cambridge, UK, and New York, NY, USA, pp. 582.

Janetos, A., Justice, C., Jahn, M., Obersteiner, M., Glauber, J., Mulhern, W., 2017. "The Risks of Multiple Breadbasket Failures in the 21st Century: a Science Research Agenda." the Frederick S. Pardee Center for the Study of the Longer-Range Future. Pardee Center Research Report.

Lassa, J.,A., Teng, P., Caballero-Anthony, M., Shrestha, M., 2018. Revisiting emergency food reserve policy and practice under disaster and extreme climate events. International Journal of Disaster Risk Science 10 (1), 1–13.

Lunt, T.A., Jones, W., Mulhern, W.S., Lezaks, D.P.M., Jahn, M.M., 2016. Vulnerabilities to agricultural production shocks: an extreme, plausible scenario for assessment of risk for the insurance sector. Climate Risk Management 13, 1–9.

Luo, Q., 2011. Temperature thresholds and crop production: a review. Climatic Change 109, 583–598.

Marx, S.M., Weber, E.U., 2012. Decision making under climate uncertainty: the power of understanding judgment and decision processes. In: Dietz, T., Bidwell, D.C. (Eds.), Climate Change in the Great Lakes Region: Navigating an Uncertain Future. MSU

Press, pp. 99–128.
National Academies of Sciences, 2016. Attribution of Extreme Weather Events in the Context of Climate Change. The National Academies Presshttps://doi.org/10.17226/21852.
Nelson, G.C., van der Mensbrugghe, D., Ahammad, H., Blanc, E., Calvin, K., Hasegawa, T., Havlik, P., Heyhoed, E., Kyle, P., Lotze-Campen, H., von Lampe, M., d'Croza, D.M., van Meij, H., Mueller, C., Reilly, J., Robertson, R., Sands, R.D., Schmitz, C., Tabeau, A., Takahashi, K., Valin, H., Willenbockel, D., 2014. "Agriculture and climate change in global scenarios: why don't the models agree. Agric. Econ. 45, 85–101.
Norwood, F.B., Lusk, J.L., 2008. Agricultural Marketing and Price Analysis. Pearson Education, Upper Saddle River, US.
OECD/FAO, 2015. Aglink-Cosimo Model Documentation: A Partial Equilibrium Model of World Agricultural Markets. " OECD Publishing, Paris.
OECD/FAO, 2018. OECD-FAO Agricultural Outlook 2018-2027. OECD Publishing, Paris/Food and Agriculture Organization of the United Nations, Rome.
Porter, J.R., Gawith, M., 1999. Temperatures and the growth and development of wheat: a review. Eur. J. Agron. 10, 23–36.
Sillmann, J., Thorarinsdottir, T., Keenlyside, N., Schaller, N., Alexander, L.V., Hegerl, G., Seneviratne, S.I., Vautard, R., Zhang, X., Zwiers, F.W., 2017. Understanding, modeling and predicting weather and climate extremes: challenges and opportunities. Weather and Climate Extremes 18, 65–74.
Stephenson, D.B., 2008. Definition, diagnosis, and origin of extreme weather and climate events. In: Diaz, H.F., Murnane, R.J. (Eds.), Climate Extremes and Society. Cambridge University Press, pp. 11–23.
Thompson, W., Smith, G., Elasri, A., 2012. World Wheat Price Volatility: Selected Scenario Analyses". OECD Food, Agriculture and Fisheries Papers, vol. 59 OECD Publishing, Paris.
Trostle, R., 2008. "Global Agricultural Supply and Demand: Factors Contributing to the Recent Increase in Food Commodity Prices." USDA Economic Research Service WRS-0801. USDA-ERS, Washington, DC.
Wiebe, K., Lotze-Campen, H., Sands, R., Tabeau, D., 2015. Climate change impacts on agriculture in 2050 under a range of plausible socioeconomic and emissions scenarios. Environ. Res. Lett. 10 (8).
Willenbockel, D., 2012. "Extreme Weather Events and Crop Price Spikes in a Changing Climate: Illustrative Global Simulation Scenarios." Research Report. Oxfam GB, pp. 60.
WMO, 2013. "2001-2010: A Decade of Climate extremes." Report No. 1103. World Meteorological Organization, Geneva, Switzerland.
Zampieri, M., Ceglar, A., Dentener, F., Toreti, A., 2017. Wheat yield loss attributable to heat waves, drought and water excess on the global, national and subnational scales. Environmental Resource Letters 12 (6), 1–11.